

Supplemental Information

Fold-Change Detection of NF- κ B at Target Genes with Different Transcript Outputs

Victor C. Wong, Shibin Mathew, Ramesh Ramji, Suzanne Gaudet, and Kathryn Miller-Jensen

Table S1. List of reactions and parameters in the D2FC model of NF-κB-induced transcription. For transcriptional reactions: h = hill function exponent, kI is the activation coefficient and kr is the repressive coefficient such that $1/kI$ is the affinity of NF-κB for the promoter and $1/kr$ is the affinity of competitor for the promoter. Parameters for which the value was scanned in a figure panel are indicated. Throughout, “NFκB” refers to a RelA-containing NF-κB dimer.

Phenomena and pertinent reactions	Parameter	Parameter value(s)	Source
TNF stimulation			
TNF	TR	$1/0 = \text{on/off}$	(1)
TNF + IKKα → IKK$\alpha(\text{active})$ + TNF	ka	Sampled, dependent on total NF-κB	(2)
Complex formation & dissociation			
Total NFκB	NF	Sampled, between 0.04 - 0.4 μM	(2)
IκBα + NFκB → IκB:NFκB	$ka1a$	$0.5 (\mu\text{M}^*\text{s})^{-1}$	(1, 3)
nIκBα + nNFκB → nIκB:NFκB	$ka1a$	$0.5 (\mu\text{M}^*\text{s})^{-1}$	(1, 3)
IκBα:NFκB → IκBα + NFκB	$kd1a$	0.05 s^{-1}	(2)
nIκBα:NFκB → nIκBα + nNFκB	$kd1a$	0.05 s^{-1}	(2)
IKK parameters			
TNF + IKKα → IKK$\alpha(\text{active})$ + TNF	ka	Sampled, dependent on total NFκB	(2)
IKKα → IKKβ	ki	0.003 s^{-1}	(1)
IKKβ → IKKγ	kp	0.0006 s^{-1}	(1)
* IKKβ → IKKγ is sensitive to A20 inhibition rate constant	$kbA20$	$0.0018 \mu\text{M}$	(1)
IKK interactions			
IKKα + IκBα → pIκBα	$kc1a$	0.074 s^{-1}	(1)
IKKα + IκBα:NFκB → pIκBα:NFκB	$kc2a$	0.370 s^{-1}	(1)
pIκBα → degradation	$kt1a$	0.1 s^{-1}	(1)
pIκBα:NFκB → degradation + NFκB	$kt2a$	0.1 s^{-1}	(1)
Transport			
NFκB → nNFκB	$ki1$	0.0026 s^{-1}	(1)
nNFκB → NFκB	$ke1$	0.000052 s^{-1}	(1)
nIκB:NFκB → IκB:NFκB	$ke2a$	0.01 s^{-1}	(1)
IκB → nIκB	$ki3a$	0.00067 s^{-1}	(1)
nIκB → IκB	$ke3a$	0.000335 s^{-1}	(1)
IκB protein synthesis and degradation			
nNFκB → nNFκB + tIκB $h = 2, kI = k^h, kr = 0; \text{ with } k = 0.065$	$cl1a$	$1.4 \times 10^{-7} (\mu\text{M}^*\text{s})^{-1}$	(1)
tIκB → tIκB + IκB	$c2a$	0.5 s^{-1}	(1)
tIκB → Degradation	$c3a$	0.0003 s^{-1}	(1)
IκB → Degradation	$c4a$	0.0005 s^{-1}	(1)
IκB:NFκB → NFκB	$c5a$	0.000022 s^{-1}	(1)
nIκB:NFκB → nNFκB	-	0 s^{-1}	(1)
A20 protein synthesis and degradation			
nNFκB + Competitor → nNFκB + Competitor + tA20 $h = 3, kI = k^h, kr = k2^h; \text{ with } k = 0.065, k2 = 0.065$	$c1$	$2 \times 10^{-7} (\mu\text{M}^*\text{s})^{-1}$	(2)
tA20 → tA20 + A20	$c2$	0.5 s^{-1}	(1)
tA20 → Degradation	$c3$	0.0004 s^{-1}	(2)
A20 → Degradation	$c4$	0.0045 s^{-1}	(1)
Prototypical inducible target transcript			
nNFκB + Competitor → nNFκB + Competitor + tIndTarget $h = 3, kI = k^h, kr = k3^h; \text{ with } k = 0.065, k3 = 0.0325 \text{ or scanned}$	$c1t$	$2 \times 10^{-7} (\mu\text{M}^*\text{s})^{-1}$ or scanned	(2)
tIndTarget → Degradation	$c3t$	0.0004 s^{-1} or scanned	(2)
Competitor protein synthesis and degradation			
nNFκB + Competitor → nNFκB + Competitor + tCompetitor $h = 3, kI = k^h, kr = k4^h; \text{ with } k = 0.065, k4 = 0.065 \text{ or scanned}$	$c1a$	$1.4 \times 10^{-7} (\mu\text{M}^*\text{s})^{-1}$	(2)
tCompetitor → tCompetitor + Competitor	$c2a$	0.5 s^{-1}	(2)
tCompetitor → Degradation	$c6a$	0.00004 s^{-1}	(2)
Competitor → Degradation	$c4a$	0.0005 s^{-1}	(2)

Sources

1. L. Ashall *et al.*, Pulsatile stimulation determines timing and specificity of NF-kappaB-dependent transcription. *Science* **324**, 242-246 (2009).
2. R. E. Lee, S. R. Walker, K. Savery, D. A. Frank, S. Gaudet, Fold change of nuclear NF-kappaB determines TNF-induced transcription in single cells. *Mol Cell* **53**, 867-879 (2014).
3. A. Hoffmann, A. Levchenko, M. L. Scott, D. Baltimore, The IκBα-NF-κB signaling module: temporal control and selective gene activation. *Science* **298**, 1241-1245 (2002).

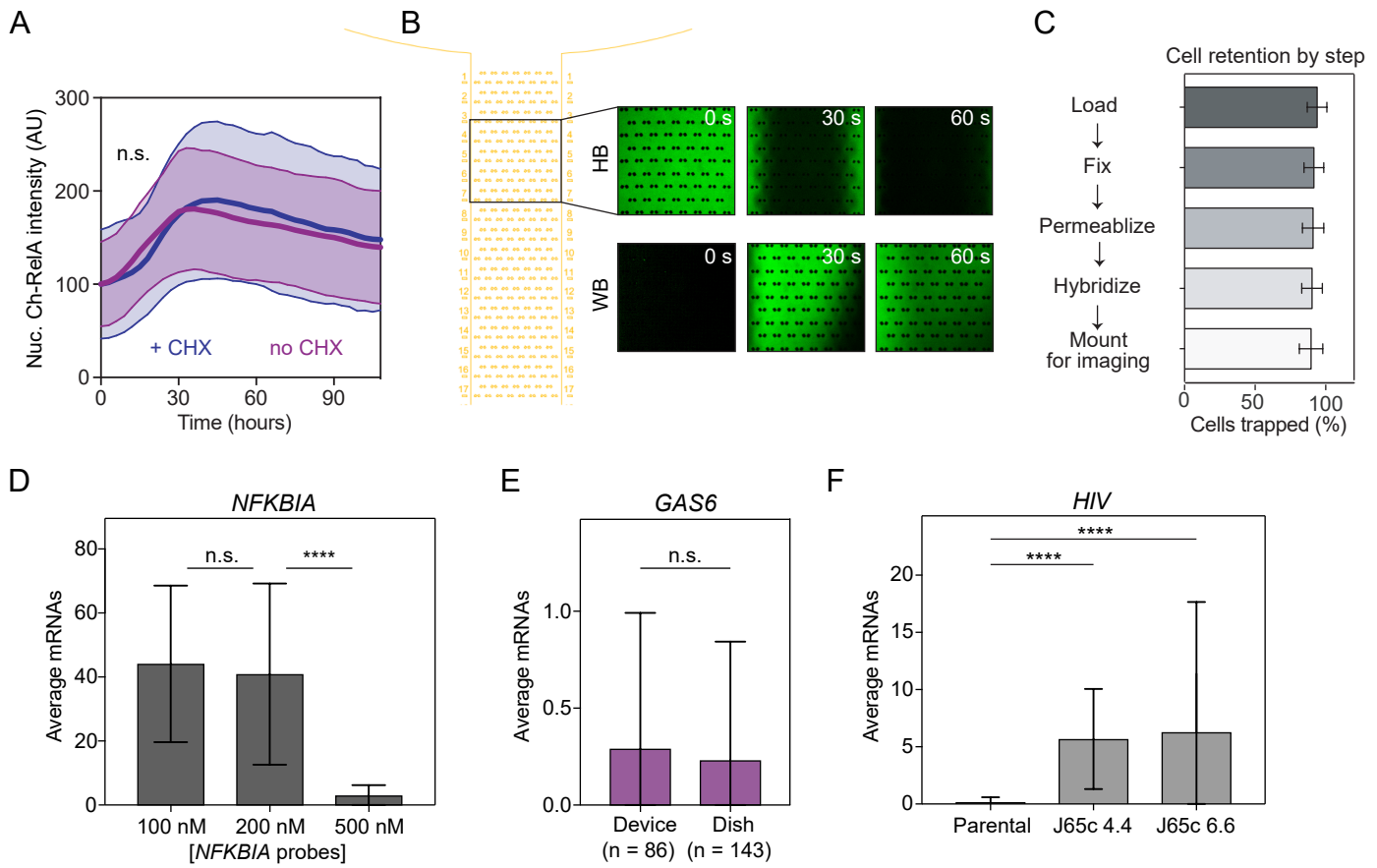


Figure S1 (related to Methods). Optimization of imaging and single-molecule RNA FISH in passive-flow device. (A) Time courses of nuclear Ch-RelA in J65c cells infected with latent HIV 6.6 collected in the passive-flow device following stimulation with 20 ng/mL TNF with 160 ng/mL CHX (blue) and without CHX (purple). Data presented as the mean \pm standard deviation (SD; shaded) of individual cell traces ($n = 30$, no CHX; $n = 44$, + CHX). No changes in cell viability were observed. Lack of statistical significance of differences in dynamics was determined by comparing distributions of t_{max} and $t_{duration}$ of the nuclear RelA intensity peak (n.s., $p > 0.05$ by Kolmogorov-Smirnov, or K-S, test). (B) Time-lapses images taken near the outlet of the passive-flow device during buffer exchanges. Buffer containing BSA conjugated with Alexa Fluor 488 is displaced from the passive-flow device channel by hybridization buffer (HB, top) within 60 seconds of adding hybridization buffer to the inlet. Similarly, the hybridization buffer is displaced from the channel by wash buffer (WB, bottom) containing BSA conjugated with Alexa Fluor 488 within 60 seconds of adding the wash buffer to the inlet. (C) Bar graph quantifying cell retention in the flow device after each step in the smFISH protocol. Fraction of cells remaining trapped after each step was determined by counting the number of trapped cells and dividing it by the total number of traps per device. Data are presented as the mean \pm SD for three devices. (D) Bar graph of mean *NFKBIA* transcripts for cells stimulated with 20 ng/mL TNF for 1 hour in the device and labelled with increasing *NFKBIA*-specific probes concentrations. Data are presented as the mean \pm SD of mRNA molecules per cell. Cell numbers: $n = 67$, 100 nM; $n = 62$, 200 nM; $n = 61$, 500 nM. (E) Bar graph of mean *GAS6* transcripts for basal cells in a tissue culture dish and in the passive-flow device. Data are presented as the mean \pm SD of mRNA molecules per cell. Cell numbers: $n = 143$, dish; $n = 86$, device. (F) Bar graph of mean HIV transcripts for HIV-infected cells and parental Jurkat cells (negative control) stimulated with 20 ng/mL TNF for 2 hours. Data are presented as the mean \pm SD of mRNA molecules per cell. Cell numbers: $n = 74$, parental; $n = 227$, J65c 4.4; $n = 211$, J65c 6.6. Statistics in (D-F) n.s. = not significant, *** $p < 0.0001$, as determined by K-S, test.

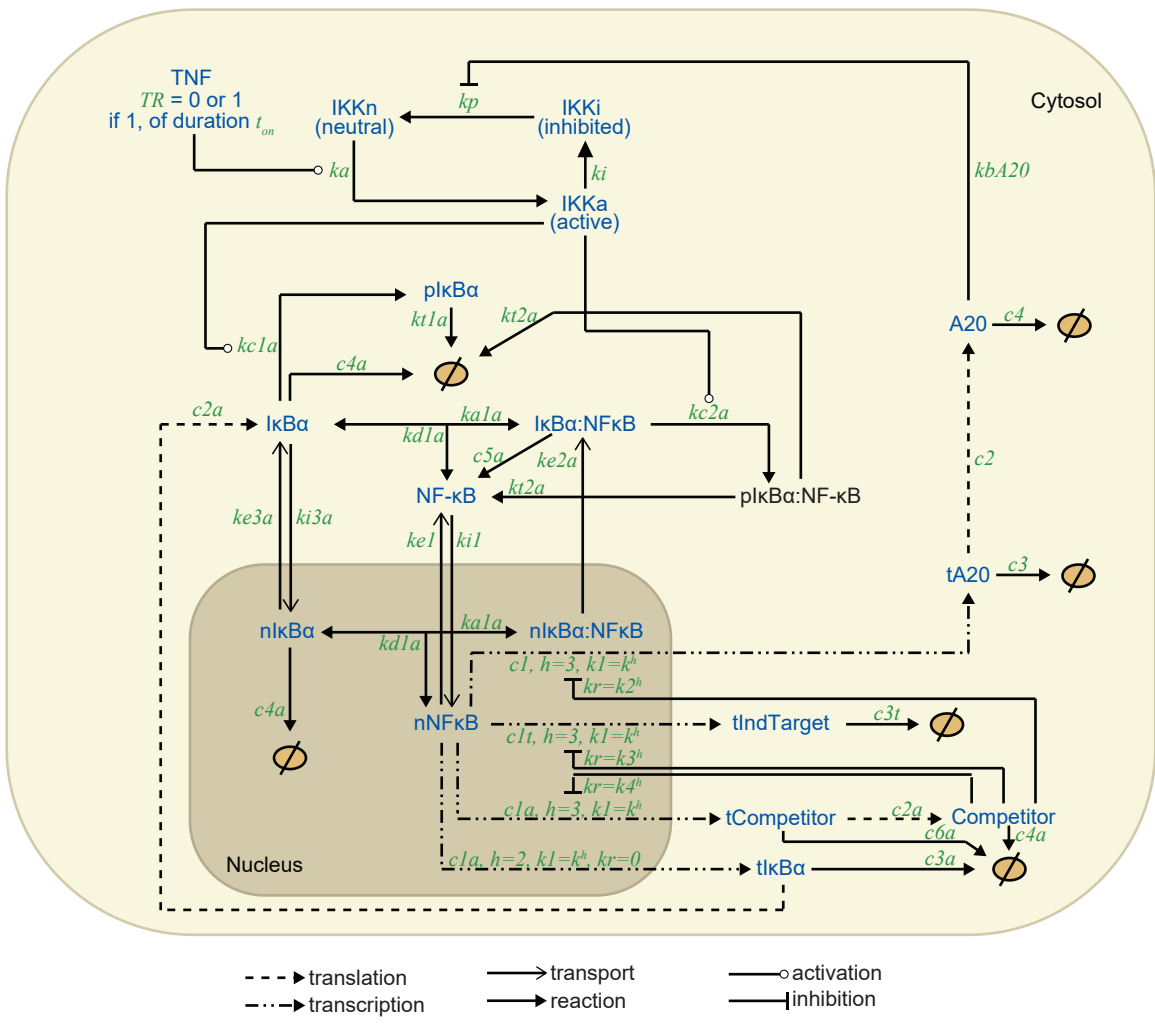


Figure S2. The D2FC model for NF-κB-dependent transcription incorporates an I1-FFL through competition on target genes promoters. Process diagram of the D2FC model. Different arrow types represent different processes or regulatory influences, reaction (binding and unbinding), transport, transcription, translation, activation or inhibition, as indicated below the diagram. Molecular species are indicated in blue, and the parameters for each reaction in green type. The model allows transport between two compartments, the cytosol and the nucleus.

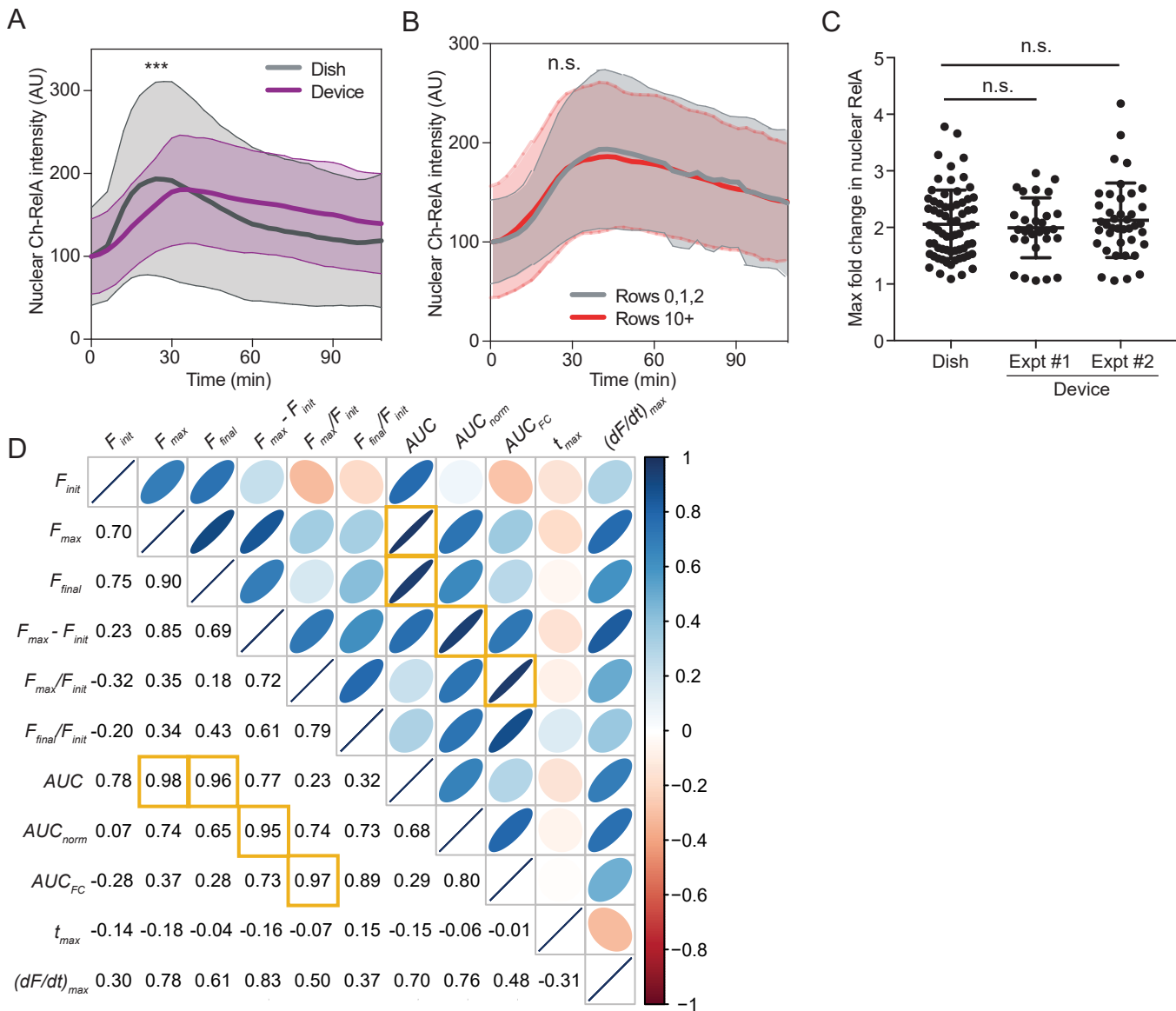


Figure S3 (related to Fig. 2). Nuclear Ch-RelA translocation dynamics show subtle differences between dish and device but max fold change in nuclear Ch-RelA does not. (A) Measured time courses of nuclear Ch-RelA from J65c cells collected in the passive-flow device (purple) versus in a tissue culture dish (gray) after 20 ng/mL TNF treatment. Data presented as the mean \pm SD of individual cell time courses ($n = 30$, device; $n = 68$, dish). (B) Measured time courses of nuclear Ch-RelA collected in the passive-flow device after 20 ng/mL TNF treatment for cells positioned in the rows 0-2 by the inlet (gray) versus rows 10+ closer to the outlet. Data presented as the mean \pm SD of individual cell time courses combined from several experiments ($n = 40$, gray; $n = 26$, red). In A-B, significant differences in dynamics were evaluated by comparing distributions of t_{max} and $t_{duration}$ of the nuclear RelA intensity peak between the two data sets (***, $p < 0.001$; n.s., $p > 0.05$ by K-S test; see Methods for more details). (C) One-dimensional scatter plots of the maximum fold change in nuclear Ch-RelA in individual cells for J65c cells in a tissue culture dish (left) or in the passive-flow device (center, right). Each dot represents an individual cell (Dish, $n = 68$, Device, Expt #1 $n = 30$ and Expt #2 $n = 39$); bars show the mean \pm SD. The distributions are not significantly different (n.s., $p > 0.05$ by K-S test). (D) Matrix of correlations between RelA signaling features extracted from the time-course data. AUC_{norm} is the area under the curve for the time course of nuclear Ch-RelA after subtraction of its initial value (time course of $F - F_{init}$). Yellow outlines mark pairwise correlations > 0.95 . Ellipses are shaped and shaded according to the direction and strength of correlation.

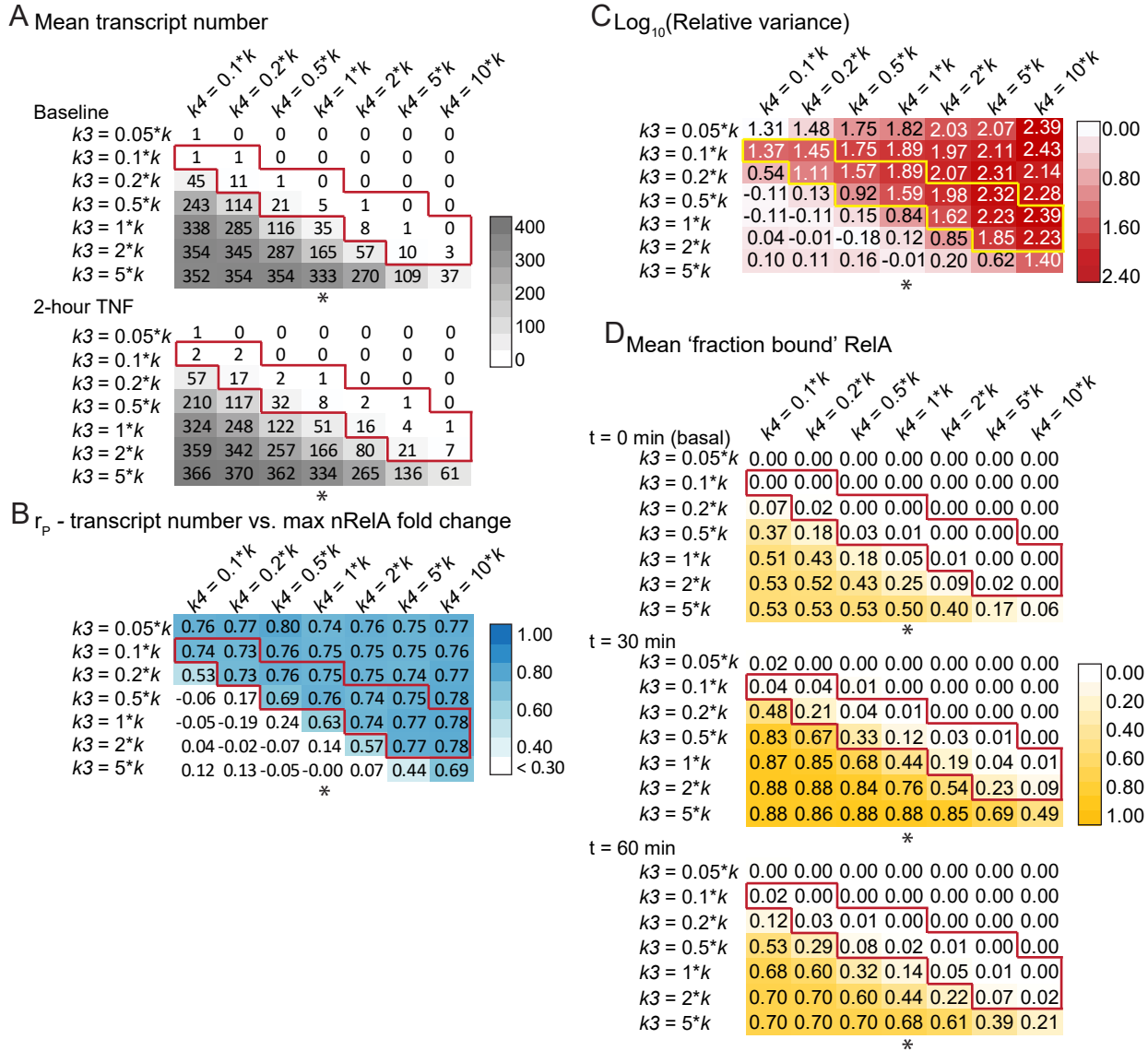


Figure S4 (related to Fig. 4). 2D parameter scan of the competitor affinity for target promoter vs. the parameter controlling competitor abundance predicts decreased RelA binding with decreasing transcript output. Heatmaps of the outputs of a parameter scan of competitor affinity (k_3 ; columns) and the parameter tuning relative competitor abundance (k_4 ; rows) producing a range of (A) median transcriptional output before and 2 hours after TNF stimulation (gray), (B) the corresponding Pearson correlation coefficients (r_p) of transcript abundance at 2 hours post-TNF with maximum fold change in nuclear RelA (blue), (C) the relative variance of transcripts before and two hours after TNF stimulation (calculated as $\log_{10}(\text{Var}_{t=120 \text{ min}}/\text{Var}_{t=0 \text{ min}})$) and (D) mean fraction of RelA bound at the target gene promoter (FB) at 0, 30, and 60 min after TNF stimulation. Both k_3 and k_4 are expressed as a function of affinity of RelA binding to a target promoter (k). The range of k_3 and k_4 combinations that correspond to our experimentally observed absolute change in transcript abundance induced by TNF at 2 hours is outlined in red in each heatmap. The asterisk marks a column discussed in Fig. 4 ($k_4 = 1^*k$).

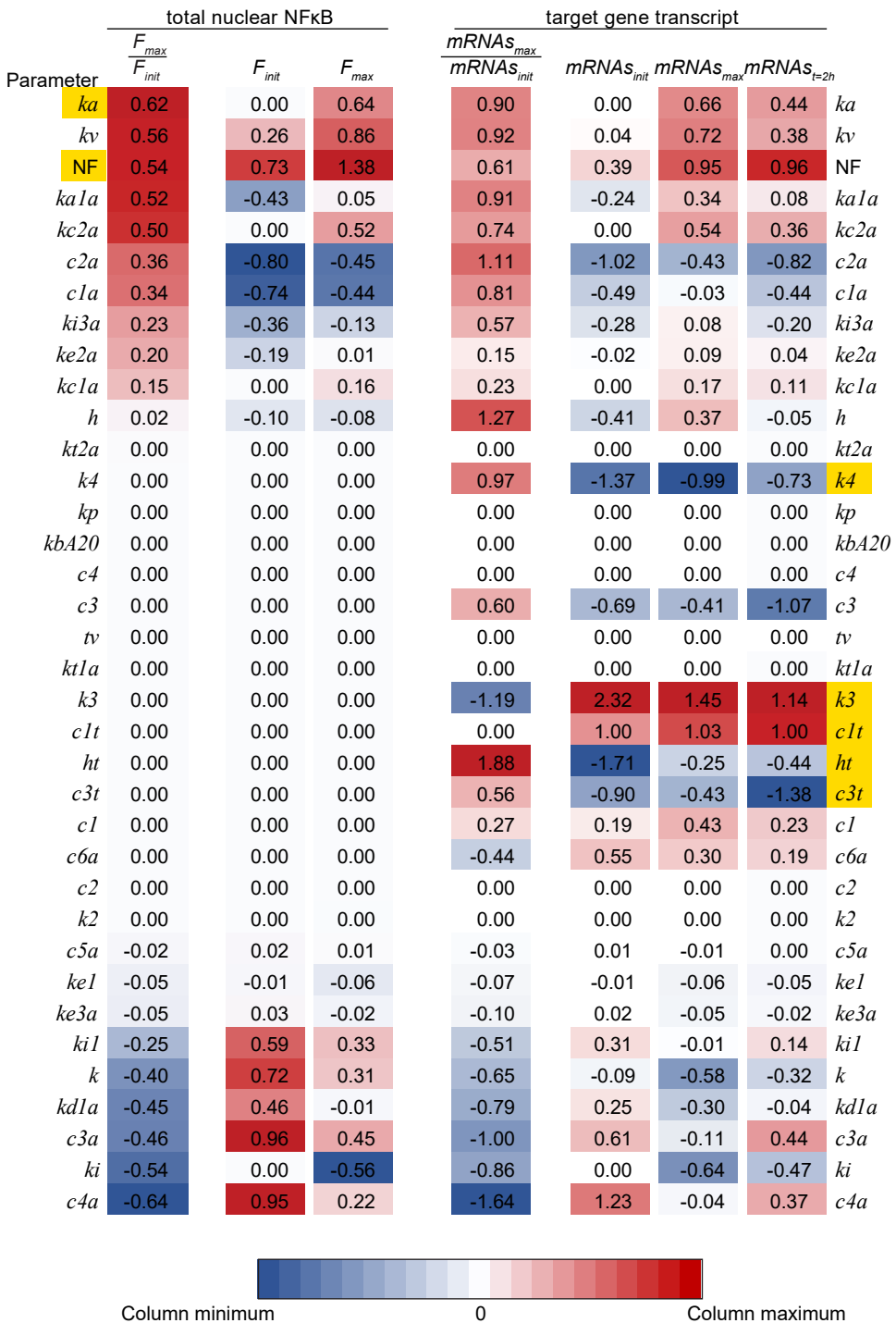
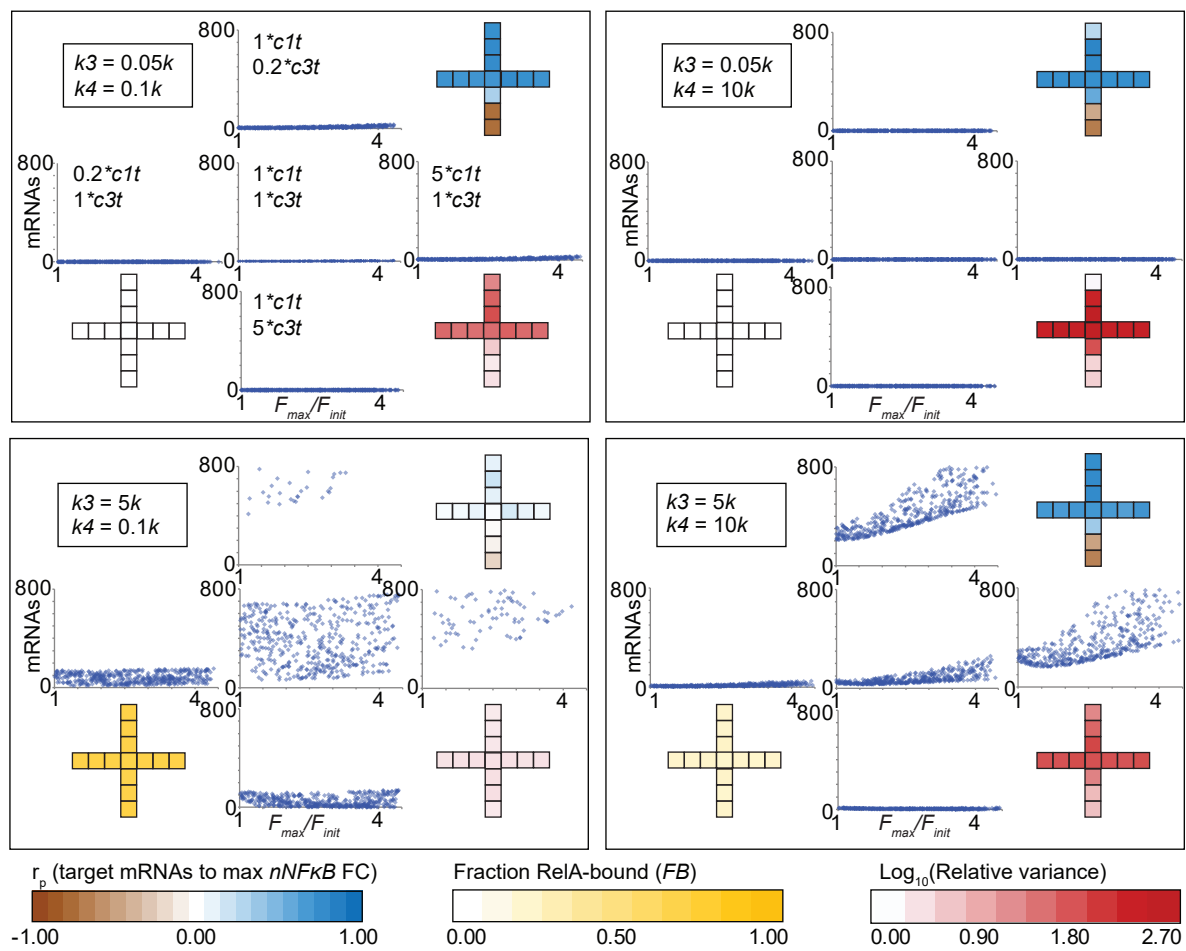


Figure S5 (related to Fig. 5). Distinct sets of parameters affect nuclear RelA dynamics and target gene transcript numbers. Heat map of the outputs of a sensitivity analysis showing the normalized local sensitivity indices for total nuclear NF- κ B (*left*) and target gene transcript (*right*) with respect to the parameters indicated for each row. For total nuclear NF- κ B, sensitivity was calculated for fold change (F_{max}/F_{init}), initial concentration (F_{init}) and maximal concentration (F_{max}). For target gene transcript, sensitivity was calculated for fold change ($mRNAs_{max}/mRNAs_{init}$), and initial ($mRNAs_{init}$), maximal ($mRNAs_{max}$) and $t = 2$ h TNF ($mRNAs_{t=2h}$) abundances. On the left, parameters highlighted in yellow were varied to mimic cell-to-cell variability (ka , NF, Figures 4, 5, 6 and S6); on the right, parameters highlighted in yellow were varied in the five-dimensional parameter scan ($k4$, $k3$, $c1t$, ht , $c3t$; Figures 5 and S6).

A



B

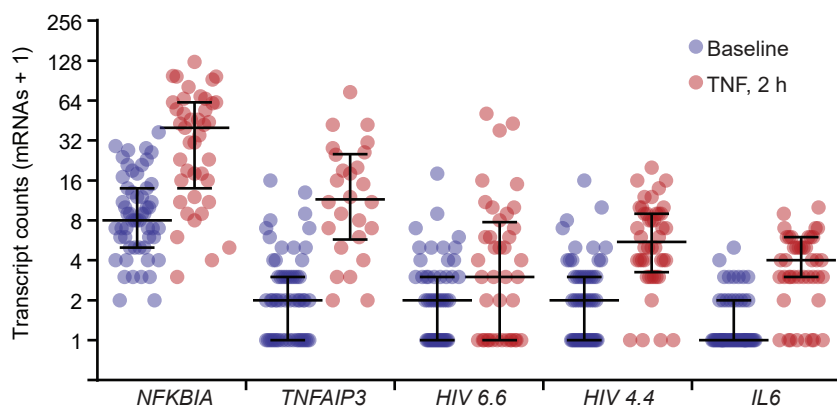


Figure S6 (related to Fig. 5). Refining parameter clouds to identify model simulations that reproduce transcript abundance, fold-change detection, and fractional RelA binding patterns observed in experiments. (A) Parameter spaces were explored for each corner of the parameter range presented in Fig. 5A (fixed k_3 and k_4 as indicated). Plots depict the simulated values of transcript number versus F_{\max}/F_{init} for nuclear RelA ($nNFkB$ in the model) for five pairs of fixed $c1t$ and $c3t$ values (as marked on the top right panel). Heat map crosses indicate the values for Pearson correlation of mRNAs at $t = 2$ h to fold change (r_p with $\text{FC} = F_{\max}/F_{\text{init}}$; brown-to-blue), the fraction RelA bound (FB ; white-to-yellow) and the relative variance (calculated as $\log_{10}(\text{Var}_{t=120 \text{ min}}/\text{Var}_{t=0 \text{ min}})$; white-to-red). (B) One-dimensional scatter plots showing the median and interquartile range (IQR) of experimental smFISH transcript numbers distributions at baseline (blue) and 2 hours after TNF stimulation (red). The IQRs were then used to identify plausible parameter sets associated with each target gene (Fig. 5B).